Hindawi
Advances in Civil Engineering
Volume 2019, Article ID 9061703, 15 pages
https://doi.org/10.1155/2019/9061703

Research Article

Comparative Investigation on Torsional Behaviour of RC Beam Strengthened with CFRP Fabric Wrapping and Near-Surface Mounted (NSM) Steel Bar

Nasih Askandar [1,2] **and Abdulkareem Mahmood** [3]

[1]*Department of Civil Engineering, Salahaddin University-Erbil, Erbil, Iraq*
[2]*Sulaimani Polytechnic University, Sulaymaniyah, Iraq*
[3]*Department of Civil Engineering, Salahaddin University, Erbil, Iraq*

Correspondence should be addressed to Nasih Askandar; nasih.askandar@spu.edu.iq

Received 24 June 2019; Accepted 7 September 2019; Published 23 September 2019

Academic Editor: Arnaud Perrot

Many researchers worldwide have extensively used fibre-reinforced polymer (FRP) strengthening materials and near-surface mounted (NSM) to enhance the shear and flexural strengths of reinforced concrete (RC) beams. However, studies on torsional strengthening are limited. Although a few studies have focused on torsional strengthening, none of them simultaneously investigated torsion with shear and/or bending moment. This study aims at demonstrating the behaviour of RC beams strengthened with FRP sheets (strips) with different configurations and NSM steel bars with different spacing that was subjected to combined actions of torsion and bending moment and making a comparison between them. Seven beams with a dimension of $15 \times 25 \times 200$ cm were casted. One of the beams was not strengthened; three of them were strengthened with carbon FRP, and the others were strengthened with NSM steel bar. The angle of twist at torque intervals, first cracking torque, ultimate torque, and ultimate twist angle of the conventional and strengthened beams during the testing process are compared. Results show a significant improvement in the torsional performance of RC beams using carbon FRP and NSM steel bar. The test beams that were strengthened with CFRP wrapping showed better enhancement in the ultimate torsional moment as opposed to the beams that were strengthened with NSM steel bar.

1. Introduction

A considerable amount of torque can accumulate in many concrete members, including curved bridge elements, spandrel beams, horizontally curved members, and eccentrically loaded beams. The torsional capacity of these members needs to be maximized due to several factors, including structural damage, deterioration, and increased loading.

Strengthening or upgrading of structural elements must be performed after a certain period to increase the service life of these elements [1, 2]. Strengthening materials can be applied to RC structures in two ways, namely, (1) the externally bonded reinforcement (EBR) method, where the strengthening materials are externally applied to the concrete surface, and (2) the near-surface mounted (NSM) method, where the strengthening materials are inserted within grooves that are pre-cut into the concrete cover [3].

Several externally bonded reinforcement (EBR) methods of increasing the service life of RC structural elements are available; for example, fibre-reinforced polymer (FRP) strengthening sheets are used to wrap RC structural elements. This technique is inexpensive and can be applied to completely degraded structures. Compared with traditional techniques, repairing concrete structures by using FRP sheets has many advantages. FRP sheets have high tensile strength, extremely low weight, high corrosion resistance, and fast installation. Moreover, changing the geometry of the structure is unnecessary when these sheets are used. This strengthening technique has already been proven to be

effective for the shear and flexural strengthening of RC beams [4–31]. A few studies focused on torsion strengthening [1, 2, 32–40].

Considered a suitable alternative to the EBR method, the NSM strengthening method involves cutting grooves in the concrete cover of a beam specimen and then inserting and embedding reinforcement into these grooves by using an adhesive. The NSM method presents numerous advantages over the EBR method, including its higher bonding productivity and better protection. The NSM method can also address the limitation of the EBR method in its maximum strain, which is below the ultimate strain due to premature debonding. The greater confinement granted by the adhesive and the surrounding concrete is considered the best advantage offered by the NSM method [41]. This strengthening technique has already been proven to be effective for the shear and flexural strengthening of RC beams [42–58]. Many studies have also used conventional steel bars instead of FRP materials for flexural and shear strengthening by employing the NSM method [59–64]. However, only few of these studies have focused on torsion strengthening [65, 66], and no previous work has investigated the application of conventional steel bars for the torsion strengthening of RC beams.

The literature review above indicates that FRP strengthening materials have been extensively used to improve the flexural and shear strengths of RC beams. NSM strengthening steel bars have also been used to improve the flexural and shear strengths of RC beams. However, studies on torsional strengthening by both techniques are limited, and none of them compared these methods for choosing the best one. Therefore, this study aims to investigate the characteristics of RC beams strengthened with both methods (FRP sheet and NSM steel bar) having different configurations under the combined actions of torsion and bending moment and making a comparison between them.

2. Materials and Testing Methods

2.1. Reinforcement and Formwork. To avoid beam failure at torsional and flexural cracking loads, each beam was designed to have a steel reinforcement ratio (ρ) of 2.3% (equation (1)) for each of the longitudinal and transverse reinforcement to the volume of concrete [33, 36, 67]:

$$\rho = \rho_{sl} + \rho_{st} = \frac{A_{sl}}{A_c} + \frac{A_t}{A_c} \cdot \frac{p_t}{s}. \quad (1)$$

The reinforcement percentage provided in a beam was higher than the minimum requirement [1] to control the integrity of the beam beyond cracking; moreover, this will reveal the case of a defective beam in terms of reinforcement. The steel reinforcement details and cross-sectional dimensions of each beam are presented in Figure 1. All beams were under-reinforced according to the American Concrete Institute code ACI 318-14 [67] to simulate torsion-deficient beams under some future loading condition. The minimum spacing of the transverse reinforcement was also purposefully exceeded to facilitate the observation of torsional failure and to hinder the stirrup from restricting the torsional cracks.

The reinforcement for the specimens included 2Φ16 and 2Φ12 mm diameter steel bars at the bottom and top, respectively. End zones that were 0.4 m long on each end of the beam were reinforced with Φ10 mm stirrups spaced at 75 mm from centre to centre to force failure in the halfway zone of the tested beam. The test region of (1.0 m) was selected in such a way that at least one complete spiral crack formed along the length of the region; therefore, Φ10 mm ($f_y = 541$ MPa) stirrups spaced at 200 mm on centres were utilised as reinforcement. Furthermore, plywood sheets (1.22 m × 2.44 m × 18 mm) were used to cast the concrete beams.

All of the RC beams used the same concrete mix with compressive strength (f_c) of 48 MPa. *Lafarge* Concrete Company (local supplier) provided the ready-mix concrete for casting the concrete beams.

2.2. Torsion Strengthening Configurations. Seven rectangular RC beams with 250 mm depth, 150 mm width, and 2000 mm length were casted by using ready-mixed concrete. The central part of these beams was specifically designed to display torsion failure. The length of the central part was set to 1.0 m to allow the formation of at least one spiral crack at the 45° angle in the longitudinal axis of these beams. One specimen was stored without strengthening and referred to as the control specimen. The strengthened beams were then divided into two groups. The first group consists of three beams and strengthened with CFRP, whilst the second group also consists of three beams and strengthened with near-surface mounted (NSM) steel bar.

2.2.1. CFRP Torsion Strengthening Configurations. CFRP composite wrap spacing was the main parameter investigated for this group. A full-wrap CFRP composite was employed to strengthen specimen 100C100. By contrast, a 100 mm width CFRP composite was used to strengthen two other beam specimens, and all-around wraps were placed at a spacing of 150 and 200 mm c/c using one layer of the CFRP composites. All beam specimens were tested under combined torsion and bending. Figure 2 shows the wrapping arrangement, and Table 1 presents the test specimen design.

2.2.2. NSM Steel Bar Torsion Strengthening Configurations. NSM groove spacing was the main parameter investigated for this group. Figure 2 presents the groove details for all three strengthened beams. Grooves 20 mm wide and 20 mm deep were cut in the 25 mm cover zone of the concrete beams, and two U-shaped conventional steel bars were embedded in these grooves. One of these steel bars had a U-shaped stirrup at the top whilst the other bar had a U-shaped stirrup at its bottom. To create an enclosed circuit stirrup, these U-shaped steel bars were welded together with at least a 100 mm overlap between their legs. The grooves were vertical (having angle of inclination of 90° with respect to the longitudinal axis of the beam). The groove spacing for these beams was set to 100, 150, and 200 mm. Sikadur-30P

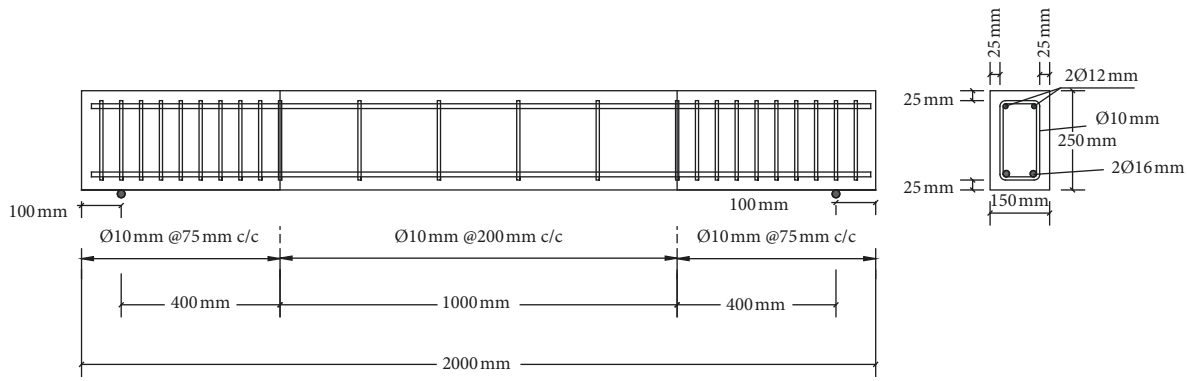

Figure 1: Dimensions and reinforcement details of the test beams.

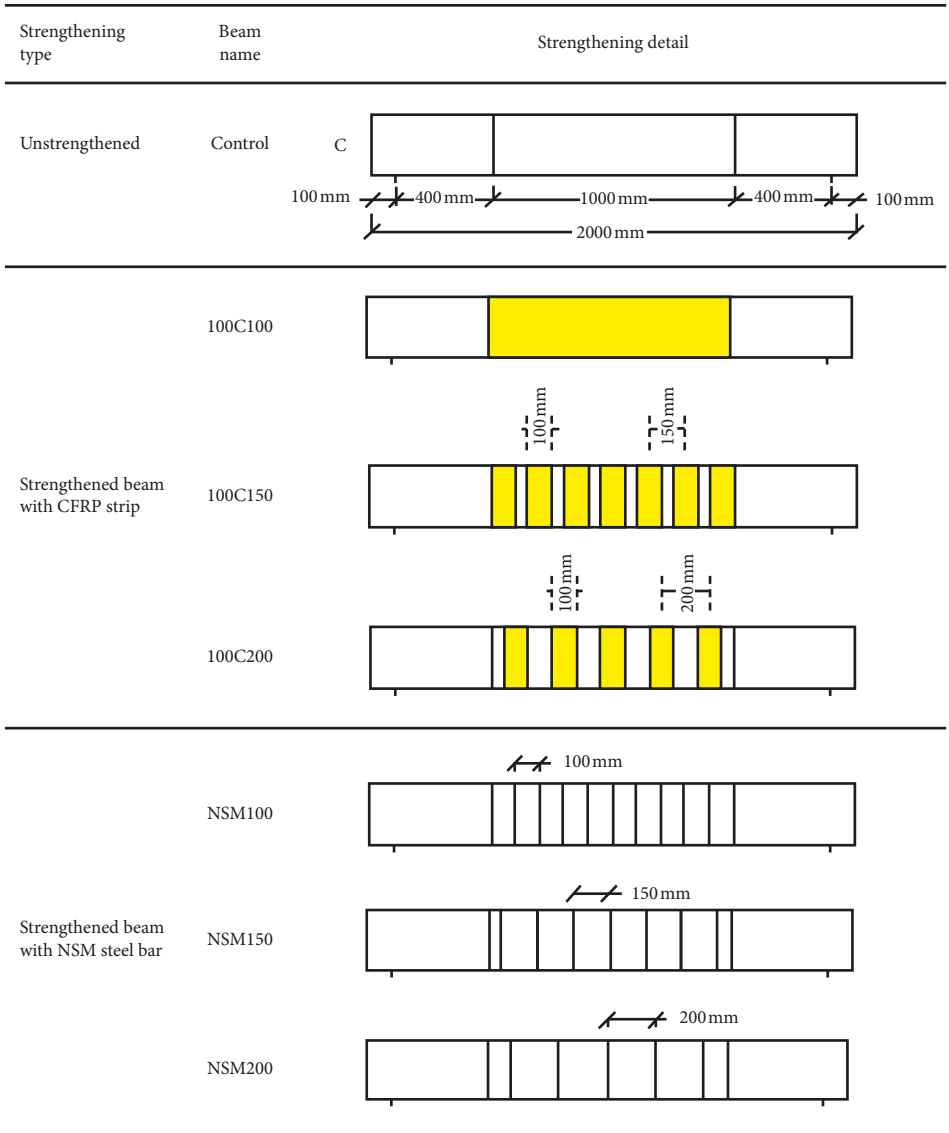

Figure 2: Strengthening of the test beams.

epoxy, a two-part epoxy that produces a clear liquid when mixed, was used as an adhesive to fill the grooves of the strengthened beams. Table 1 lists the information related to this system.

2.3. FRP Material

2.3.1. CFRP Material Properties. The experiment used carbon fibre fabric SikaWrap®-300C and epoxy-based saturated

Table 1: Design of the concrete beams.

Beams	Strengthening technique	CFRP transverse strip			NSM steel bar spacing (mm)
		No. of layers	Width (mm)	Spacing (mm)	
Control		Unstrengthened			
100C100 (full wrap)		1	Full		—
100C150	CFRP sheet	1	100	150	—
100C200		1	100	200	—
NSM100		—	—	—	100
NSM150	NSM steel bar	—	—	—	150
NSM200		—	—	—	200

resin Sikadur-330. Unidirectional CFRP fabrics (SikaWrap-300C) with a thickness of 0.166 mm per ply were also utilised. The elastic modulus, ultimate tensile strength, and elongation at failure of the fibre were 230 GPa, 3900 MPa, and 15 mm/m, respectively, according to the manufacturer. The FRP sheets were bonded to concrete by using two pieces of "rubber-toughened cold-curing-construction epoxy adhesive (Sikadur-330)" with a density, elastic modulus, and tensile strength of 1310 kg/m^3, 3800 MPa, and 30 MPa, respectively. Tables 2 and 3 list the information related to this system.

2.3.2. Preparing and Installing CFRP. The bond between the RC beam and CFRP was given appropriate attention during the strengthening process. When fixing the CFRP to the concrete surface, a handheld grinder was utilised to level the concrete surface disclosing the aggregate. The grinder was used again to arciform the concrete corners to a minimum radius of 13 mm [3] and reduce the stress concentration in the fibres at the edges. This stress concentration will lead to rupture failure of CFRP sheets at corner edges before reaching their ultimate strength. Water and compressed air were used to clean the concrete surface from released particles and dirt.

2.3.3. Applying CFRP to the Concrete Substrate Surface Was Regulated in Steps. The beams were cleaned by washing with pressurized water and allowed to dry prior to CFRP sheet application. Loose particles and defilements from the specimen's surface were removed by this procedure. The beams were also wire brushed and vacuumed prior to the CFRP sheet application. Depending on substrate roughness, the resin (Sikadur-330) was mixed and applied to the prepared concrete surface by using a brush at the amount of approximately 0.75 kg/m^2 to 1.25 kg/m^2. The SikaWrap®-300C sheet was cut into strips with 100 mm width by scissors for the required length for all the specimens (estimated overlap greater than 150 mm). The (SikaWrap®-300C) strip was applied to the resin with a special plastic roller until the resin was squeezed out between the roving. Then, the SikaWrap®-300C fabric was applied onto the resin coating in the appropriate direction.

2.3.4. FRP Ratio as Transverse Reinforcement. Figure 3 presents the FRP ratios for the strengthened beams (group 1). Equation (2) was used to calculate the volumetric ratios of CFRP reinforcement, ρ_f [34, 35]:

Table 2: SikaWrap®-300C (woven carbon fibre fabric for structural strengthening).

Characteristics	Note
Fibre type	Midstrength carbon fibres
Fibre orientation	0° (unidirectional)
Areal weight	300 ± 15 g/m^2
Fabric design thickness	0.166 mm (based on fibre content)
Tensile strength of fibres	3,900 N/mm^2 (nominal)
Thickness	1.3 mm per layer (impregnated with Sikadur®-330) 1.0 mm per layer (impregnated with Sikadur®-300)
Tensile E-modulus	230,000 N/mm^2
Elongation at break	1.5% (nominal)

Table 3: Sikadur-330 (two-part epoxy impregnation resin).

Appearance and colours	Resin part A: white (paste); hardener part B: grey (paste)
Density	1.31 kg/l (mixed)
Mixing ratio	A : B = 4 : 1 by weight
Open time	30 min (at + 35°C)
Viscosity	Pasty, not flowable
Service temperature	−40°C to +50°C
Tensile strength	30 MPa (cured seven days at +23°C)
Flexural E-modulus	3800 MPa (cured seven days at +23°C)

$$\rho_f = \frac{n_f t_{fd} b_f P_f}{A_c s_f}. \quad (2)$$

2.4. NSM Steel Bar Strengthening Technique

2.4.1. NSM Steel Bar Materials. Ready-mixed concrete also was used for all three beams in this group. The compressive strength (f'_c) of the supplied concrete was evaluated after 28 days. The average results of three concrete cylinders (100 mm in diameter and 200 mm in height) on the day of the testing were considered for computing the compressive strength. Sikadur-30P epoxy, a two-part epoxy that produces a clear liquid when mixed, was used as an adhesive to fill the grooves of the strengthened beams.

Three bars with similar diameters and three welded bars (Ø10 mm) were subjected to uniaxial tensile tests to determine their yield and ultimate strength (f_y, f_u)

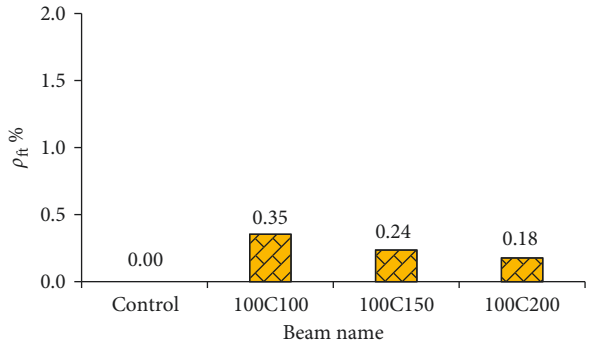

Figure 3: CFRP sheet reinforcement ratios for the strengthened beams.

following the recommendations of ASTM A370-10 2010 [28].

Table 4 summarizes the mechanical properties of the concrete and NSM steel bars, the average compressive strength of the concrete (f'_c), and the average test results for the steel bars, whilst Table 5 presents the properties of the epoxy based on the specifications supplied by the manufacturer.

2.4.2. NSM Steel Reinforcement Ratio. The NSM steel reinforcement ratios for the strengthened beams in this group are shown in Figure 4. CFRP sheet and NSM steel reinforcement ratios for the strengthened beams for both groups are shown in Figure 5. The volumetric ratios of NSM steel bar reinforcement, ρ_{nst}, were calculated by using the following equation:

$$\rho_{nst} = \frac{\text{vlume of steel stirrup}}{\text{Volume of concrete}} = \frac{A_{nst}p_{nst}}{A_c S}. \quad (3)$$

2.4.3. Specimen Preparation. The installation of the strengthening steel bars began by cutting grooves into the concrete cover of the specimens after 28 days of curing. These grooves were cut in the transversal direction around the beam cross section, whilst maintaining dimensions greater than 1.5 db × 1.5 db (where db denotes the diameter of the NSM steel reinforcement). A special concrete saw (handle grinder) with a diamond cutting saw blade was used for the cutting. A hammer drill and chisel were used to remove any remaining concrete lugs and to roughen the lower surface of the grooves. These grooves were then smoothened and cleaned with a wire brush and a high-pressure air jet. The strengthening steel bars were bent into a U-shape, and two U-shaped steel bars were used for each closed groove (one at the top and the other at the bottom). In this way, these steel bars were overlapping for approximately 100 mm and welded together to form a closed stirrup at each round groove. These grooves were then filled with an epoxy adhesive groove filler (Sikadur-30 LP) around the steel bar and the surface was levelled as shown in Figure 6. To ensure that the epoxy reached its full strength, the beam was kept for at least two weeks of curing time.

Table 4: Mechanical properties of the concrete and NSM steel bars.

Material	Compressive strength (MPa)	Yielding tensile strength (MPa)
Concrete	48	—
Steel bars Ø10 mm	—	541
Welding steel bars Ø10 mm	—	298

Table 5: Sikadur®-30 LP (two-part epoxy impregnation resin).

Appearance and colours	Part A: white; Part B: black; parts A + B: light grey
Density (at 23°C)	~1.65 kg/lt (parts A + B)
Mixing ratio	Part A : B = 3 : 1 by weight or volume
Layer thickness	30 mm max
Open time	90 minutes (at +25°C)
Viscosity	Pasty, not flowable
Service temperature	−40°C to +45°C (when cured at >+23°C)
Tensile strength	15 MPa to 18 MPa (when cured for seven days at +23°C)
Shear strength	17 MPa to 21 MPa [+40°C to +55°C (7 days)]

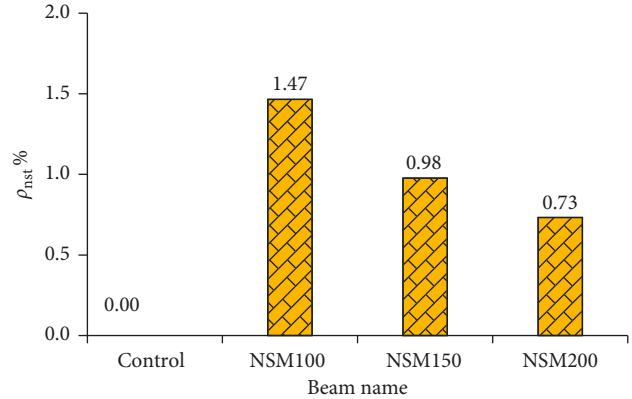

Figure 4: NSM steel reinforcement ratios for the strengthened beams.

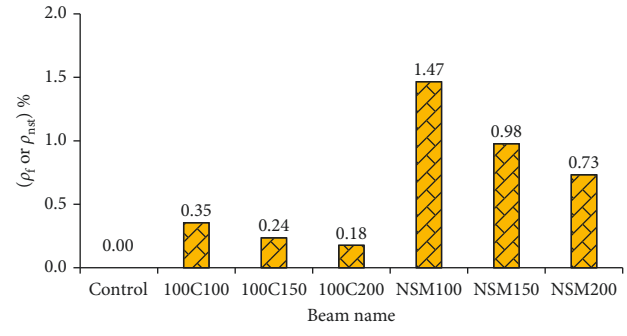

Figure 5: CFRP sheet and NSM steel reinforcement ratios for the strengthened beams.

2.5. Test Setup and Instrumentation. Figure 7 shows the details of the test setup. The load at the active support was applied using a 200 ton hydraulic jack. The jack had a 500 mm lever arm from the centroidal beam axis. The periodical applied load was measured using a compression

Figure 6: Grooving, NSN steel bar installation, welding, and groove filling with epoxy.

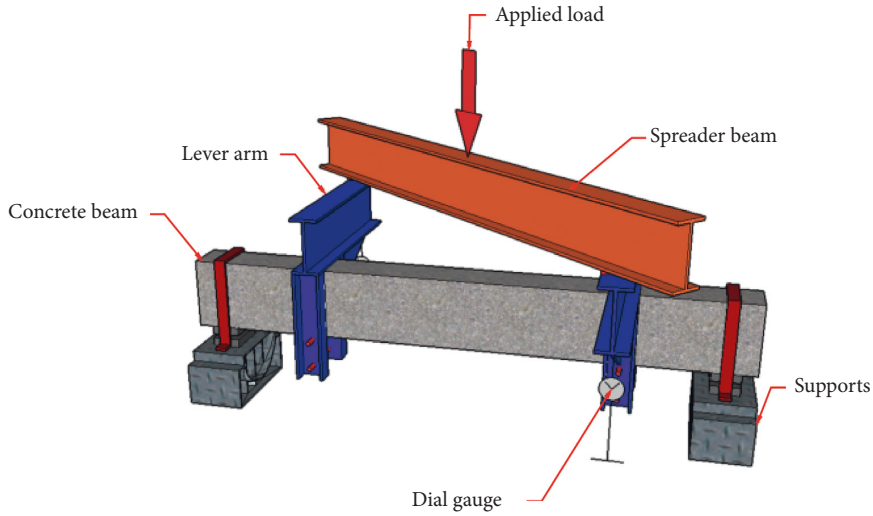

Figure 7: Schematic of the test setup for applying combined torsion and bending.

load cell with a 100 ton capacity. The hydraulic jack had a movable length of 250 mm, thus providing a 57.3° twist capacity for the beam. The reaction arm had 500 mm eccentricity from the centroidal axis of the beam. The beam elongated longitudinally after cracking and was allowed to slide and elongate freely to avoid any longitudinal restriction and consequent compression. This feature was obtained by supporting the beam ends on rollers at the unresisting support. The twist angle of the free end (the point of applying torque) was measured by a dial gauge with the aid of the downward distance of the lever arm at that point.

Load application on the beam specimens to be tested under the combined action of torsion and bending utilised a fabricated loading frame from the civil engineering laboratory. Rotation around the longitudinal beam axis was arranged via a special support condition, and lever arms were attached to the specimen to provide a torsional moment, as shown in Figure 7. The specimen underwent pure torsion when the location of a lever arm coincided with the support. The lever arm was maintained beyond the two supports to apply combined bending and torsion.

(i) Three dial gauges were used. Two of them for measuring displacements were positioned under the lever arm, and one was placed at the centre to measure central displacement.

(ii) A distance of 400 mm was maintained between the centre of the support and lever arm to achieve bending and torsion.

(iii) The load of the hydraulic jack was transferred to the specimen through a spreader beam resting on the end of a lever arm attached to the specimen. Thus, half of the applied load acted at the end of each lever arm.

(iv) The length of the specimen between supports was 1.8 m, with 0.1 m projection outside the support. The central 1.0 m length of the specimen was subjected to combined bending and torsion, whereas 0.4 m length of the beam near each support was subjected to bending moment and shear force. The torque in the middle part of the specimen was the product of the load at the end of each lever arm (half the total of applied load) multiplied by the length of the lever arm from the centre of the specimen. The twist angle at each lever arm was achieved from a vertical displacement of a lever arm end point and length of the lever arm. The overall twist angle in the middle part of the specimen was equal to the sum of twist angles at the couple of the lever arm.

2.6. Test Procedure. Figure 8 shows the hydraulic testing machine in the civil engineering laboratory that was utilised to test the beam specimens.

The circular rotation of the supports and the transmission of applied load from the centre of the machine to the two points that express the moment arm must be facilitated by the experimental conditions. Figures 7 and 8 show the particular clamping loading frame used in this study. This frame consisted of an I-section (200 mm × 80 mm × 8 mm) attached to two steel channels (100 mm × 50 mm × 8 mm) by welding. After insertion around the beam cross section by large bolts, these steel channels connect from the bottom, and each arm utilises two bolts. Attached steel clamps work as lever arms for applied torque with separated faces to connect them over the sample. The final shape is similar to a bracket. These lever arms are suitable for providing the required eccentricity of 500 mm with respect to the longitudinal axis. As shown in Figures 7 and 8 the transmission of the loads from the centre of the machine to the two lever arms was achieved using an I-section steel spreader beam with 200 mm depth and 2 m length. Increment readings at each load were acquired through recorded camera videos, strains from the data logger, and cracks were recorded in accordance with their occurrence.

2.7. Angle of Twist Measurements. As shown in Figure 9, a dial gauge connected to the bottom of a lever arm at a point (500 mm) from the centre of the longitudinal axis of the beam was used to evaluate the angle of twist. The downward value of the lever arm was recorded by the dial gauge to determine the twist angle in radians.

3. Results and Discussion

Table 6 shows a summary of the cracking torque (T_{cr}), ultimate torque (T_u), and ultimate twist angle (θ_u) of the concrete beams. Overall, the results demonstrate the significant improvement of T_{cr}, T_u, and θ_u of the concrete beams with the use of FRP sheets and NSM steel bar.

3.1. Ultimate Torsional Moment Carrying Capacity. The ultimate torsional moment carrying capacity of the control and strengthened beams are shown in Figure 10. Nonlinear improvement of the ultimate torsional moment carrying capacity of the strengthened beams in relation to the control beam, especially for beams that were strengthened with NSM method, was also observed. The strengthening method and materials used were mainly affecting the improvement rather than FRP strip and NSM steel bar spacing. The maximum ultimate torsional moment of 25.15 kN·m was demonstrated by beam 100C100, and beam NSM200 showed the minimum torsional moment of 14.35 kN·m. The values for the other strengthened beams were between those of the two beams. Ultimate torsional moment for beams 100C150, 100C200, NSM150, and NSM200 were 21.85, 19.88, 15.50, and 14.75 kN·m, respectively.

3.2. Influence of Material and Techniques Used for Strengthening on Torsional Strength. The ultimate torsional moment carrying capacity of the control and strengthened beams with respect to the strengthening material (CFRP sheet and NSM steel bar) and reinforcement ratio are shown in Figure 11. Nonlinear improvement of the ultimate torsional moment carrying capacity of the strengthened beams in relation to the control beam was also observed. The strengthening material and techniques used mainly influenced the improvement.

The percentage of enhancement in the ultimate torsional moment (T_u) for beams 100C100 and NSM100, with the same spacing but with different strengthening technique and material and with strengthening material reinforcement ratio of 0.35% and 1.47%, is 134% and 44%, respectively.

The percentage of enhancement in the ultimate torsional moment (T_u) with respect to the control specimen for beams 100C150 and NSM150, with 150 mm spacing and strengthening material reinforcement ratio of 0.24% and

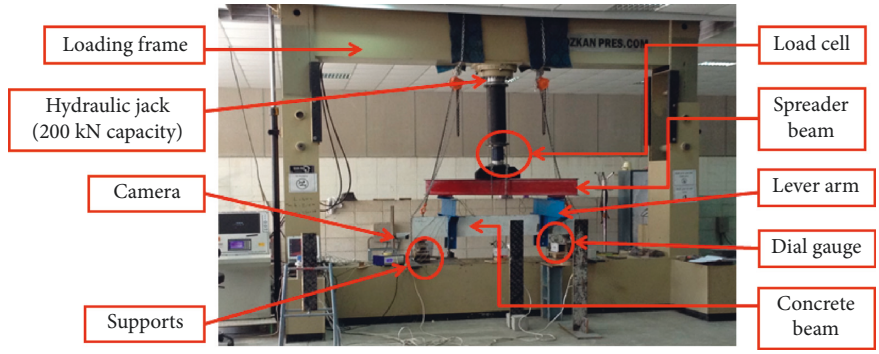

Figure 8: Test setup with the loading frame.

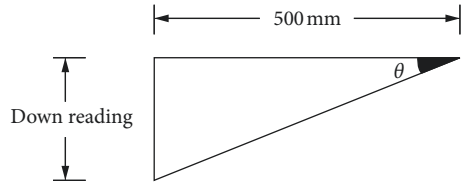

Figure 9: Angle of twist measurements.

Table 6: Experimental results of the tested beams.

Beam code	Str. Tech.	f_c' MPa	T_{cr} kN·m	%Incr.T_{cr}	T_u kN·m	%Incr.T_u	θ_u deg./m	%Inc. θ_u
Control	Un-str.		4.50	—	10.75	0	4.77	0
100C100			N.A	—	25.15	134	10.49	120
100C150	CFRP sheet		7.75	72	21.85	103	10.39	118
100C200		48	7.00	56	19.88	85	9.17	92
NSM100			8.50	89	15.50	44	3.97	−17
NSM150	NSM steel bar		8.00	78	14.75	37	3.64	−24
NSM200			7.00	56	14.35	33	3.47	−27

Str. Tech.: strengthening technique; %Incr.T_{cr}: increase of cracking torque in percentage; %Incr.T_u: increase of ultimate torque in percentage; %Incr. θ_u: increase of ultimate twist angle in percentage; Un-str.: Unstrengthened.

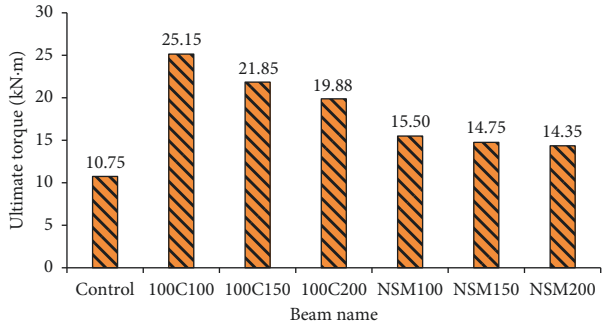

Figure 10: Ultimate torsional moment carrying capacity.

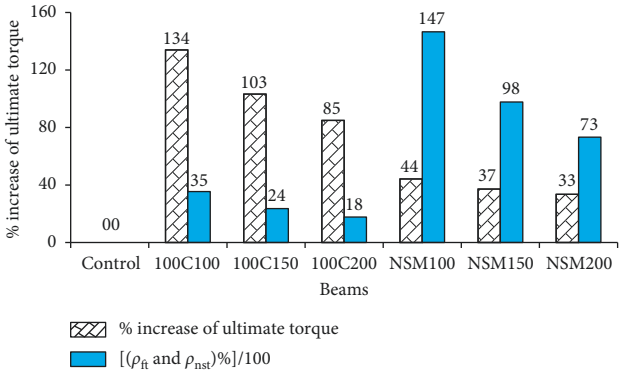

Figure 11: FRP and NSM steel reinforcement ratios and increase in ultimate torque in percentage.

0.98%, is 103% and 37%, respectively. While this percentage for beams 100C200 and NSM200, with 200 mm spacing and strengthening material reinforcement ratio of 0.18% and 0.73%, is 85% and 33%, respectively.

3.3. Influence of Strengthening Method on Beam Ductility. The ultimate twist angle carrying capacity of the control and strengthened beams are shown in Figure 12. The strengthening method and materials used were mainly influencing the ductility of the strengthened beams. Beams that were strengthened with CFRP sheet represented more ductility than the control beam, and the others were strengthened with NSM steel bar. Beams 100C100, 100C150, and 100C200 that were strengthened with CFRP sheet, the

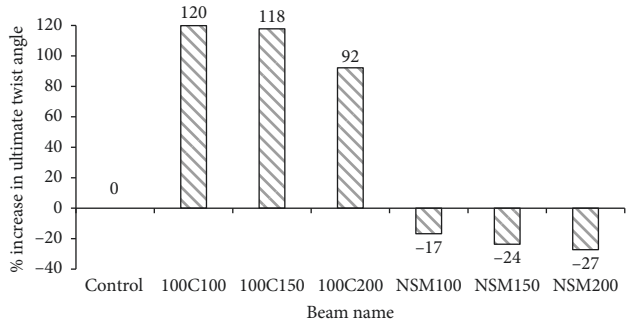

Figure 12: Enhancement percentage of the ultimate twist angle carrying capacity.

enhancement percentage of their ultimate twist angle (θ_u) with respect to the control beam was 120%, 118%, and 92%, respectively, whilst beams NSM100, NSM150, and NSM200 that were strengthened with NSM steel bar, the diminution percentage of their ultimate twist angle (θ_u) with respect to the control beam was 17%, 24%, and 27%, respectively.

3.4. Influence of CFRP and NSM Steel Bar Spacing on the Torsional Strength. Figure 13 shows the influence of CFRP and NSM steel bar spacing on the enhancement percentage of ultimate torsional strength of the strengthened beams with respect to the control beam. The spacing of CFRP sheets for beams that were strengthened with CFRP sheet had a great effect on enhancement percentage of ultimate torsional strength of the strengthened beams than that beams strengthened with NSM steel bar.

The enhancement percentage of the ultimate torsional moment (T_u) of beams 100C100, 100C150, and 100C200 that were strengthened with CFRP sheet and spacing of 100, 150, and 200 mm is 134%, 103%, and 85%, respectively, whilst its value for beams NSM100, NSM150, and NSM200 with the same spacing but with NSM steel bar strengthening method is 44%, 37%, and 33%, respectively.

3.5. Torque-Twist Comparison. Figure 14 shows the torque-twist behaviour of the control and strengthened beams. Utilising CFRP sheets for the same load, the control beam had a smaller torque carrying capacity and higher twist angle values compared with the strengthened beams. Amongst all of the strengthened beams, 100C100 and 100C150 exhibited the best ductility. Furthermore, the tendency of the torque-twist angle of all the beams did not significantly change before cracking occurred. Owing to the stirrup, external CFRP strips or NSM steel bar that exhibited torque resistance in the post-cracking stage, all curves showed a reliable slope to reach the ultimate torque of beams. Therefore, an increase in torsional rigidity of the beams was observed, and the loading stopped after reaching the ultimate torque.

3.6. Crack Pattern and Failure Modes. Figure 15 shows the failure modes of the unstrengthened (control) and CFRP-strengthened RC beams under combined bending and torsion. The torsional moment resulted in the failure of all

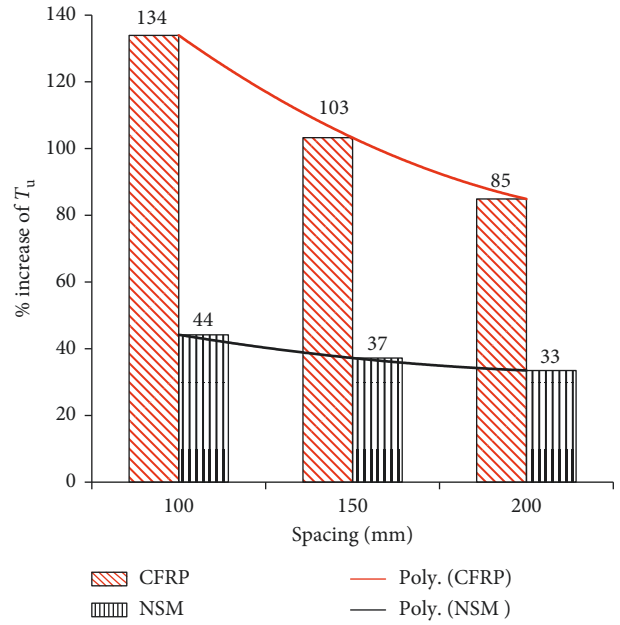

Figure 13: Influence of CFRP and NSM steel bar spacing on the torsional strength.

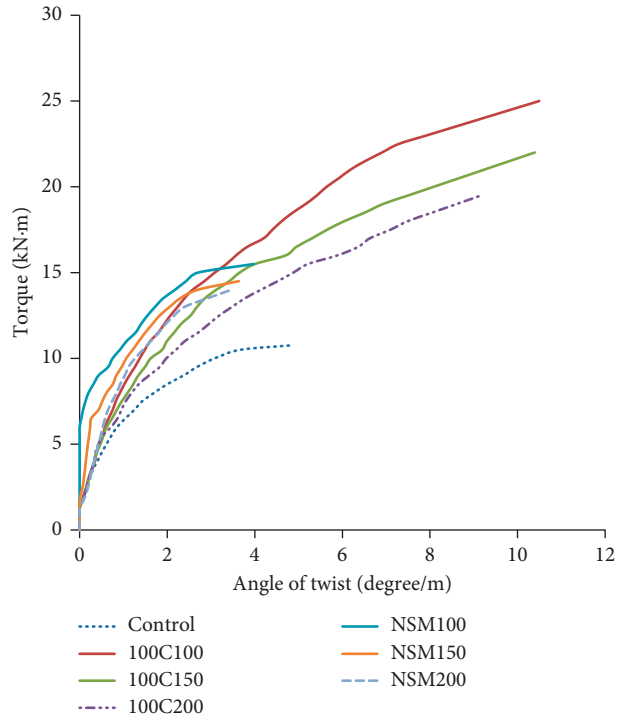

Figure 14: Torque versus angle of twist at each concrete beam.

the tested beams. The number of cracks in the strengthened beams was larger than that in the control beam; thus, the strengthened beams had higher tensile stress. The emergence of flexural cracks was observed in the control beam at the midlength of one or both of the beam vertical faces. Tension cracks generated and propagated in a spiral form. The cracks gradually widened as the load increased,

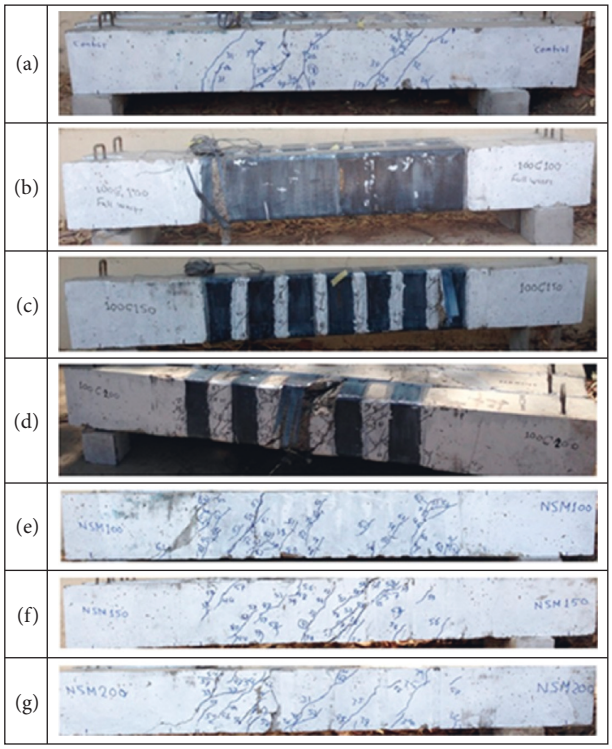

Figure 15: Mode of failure for specimens tested under combined torsion and bending. (a) Control specimen, (b) full transverse wrapping (100C100), (c) 100C150, (d) 100C200, (e) NSM100, (f) NSM150, (g) NSM200.

with the two lever arms rotating relative to one another around the RC beam centroidal axis along with bending. Most of the concrete cracks in the strengthened beams were dispersed through the concrete surfaces between the FRP strips and NSM steel bar grooves. In addition, fibre failure in specimen 100C100 was observed from the edge of the central portion of the beam specimen, and sudden failure of the RC beam occurred after the emergence of the first fibre crack. The FRP sheets ruptured after concrete cracking in specimens 100C150 and 100C200. In NSM100, the first crack appeared at the edge of the test region in both sides near the lever arm. This crack propagated very slowly and dispersed throughout the test region in a spiral formation immediately before the failure caused by the main crack near the lever arm was widened to approximately 6 mm. For NSM150, the first crack appeared at the centre of the test region and in both sides of the specimen; these cracks propagated and dispersed throughout the central portion of the test region in a spiral formation, and the widening of the main crack at the centre of the test region resulted in a failure. For NSM200, the first crack appeared at a quarter length in both sides of the test region and resulted in a failure.

4. Analytical Predictions

4.1. CFRP-Strengthened Beams. The full torsional strength of CFRP-strengthened RC beams can be analysed by the design codes using the principle of superposition from both the CFRP and steel reinforcement.

The ultimate torsional strength for the FRP-strengthened tested beams, T_u, can be achieved by adding the contribution due to fibres and due to reinforced concrete beam, as follows:

$$T_u = T_{u,RC} + T_{u,FRP}. \tag{4}$$

The design equation to calculate the ultimate torsional strength of a reinforced concrete beam, $T_{u,RC}$, recommended by [67, 68] is as follows:

$$T_{u,RC} = T_T + T_L, \tag{5}$$

$$T_T = \frac{2(0.85) \cdot A_o \cdot A_t \cdot f_{yv}}{S}, \tag{5a}$$

$$T_L = \frac{2A_o \cdot A_{sl} \cdot f_{sl}}{P_o} \tan\theta, \tag{5b}$$

$$\tan\theta = \sqrt{\frac{A_t \cdot f_{st} \cdot P_o}{A_{sl} \cdot f_{sl} \cdot S}}. \tag{5c}$$

FIB Bulletin-14, 2001 design model [69] states that an externally bonded FRP laminate will grant contribution to the torsional capacity only if full wrapping around the beam's cross section is applied, so that the tensile forces carried by the FRP on each side of the cross section may create a continuous loop. The technical document also provides for the possibility of using inclined FRP strips as a strengthening solution. Based on the assumption of the validity of the truss mechanism, the following equations (6)–(8) were provided to predict the FRP contribution to strength $T_{u,FRP}$:

$$T_{u,FRP} = 2\varepsilon_{fk,e} E_{fu} \frac{t_f b_f}{S_f} bh \cdot \cot\theta, \tag{6}$$

$$\varepsilon_{fk,e} = 0.8\varepsilon_{fe}, \tag{7}$$

$$\varepsilon_{fe} = 0.17 \left(\frac{f_c'^{2/3}}{E_{fu}\rho_f} \right)^{0.3} \varepsilon_{fu}. \tag{8}$$

Equation (2) was used to calculate the volumetric ratios of CFRP reinforcement, ρ_f [34, 35].

4.2. NSM Steel Bar-Strengthened Beams. The full torsional strength of the NSM-strengthened RC beams can be analysed by the design codes using the superposition principle of both the NSM steel bar and internal steel stirrups.

The T_u of the NSM-strengthened tested beams can be calculated as follows by adding the contributions of the NSM steel bar and the reinforced concrete beam:

$$T_u = T_{u,RC} + T_{u,NSM}. \tag{9}$$

$T_{u,RC}$ is calculated as follows following the recommendations of [67, 68]:

Table 7: Comparison of the experimental and analytical ultimate torsional moments.

Beam code	Ultimate torsional moment T_u (kN·m)		$T_{u,Exp.}/T_{u,An}$
	Experimental	Analytical	
Control	10.75	13.32	0.81
100C100 (full wrap)	25.15	26.23	0.96
100C150	21.85	24.83	0.88
100C200	19.88	20.13	0.99
NSM100	15.50	25.95	0.60
NSM150	14.75	21.13	0.70
NSM200	14.35	18.08	0.79

$T_{u,Exp.}$: experimental ultimate torsional moment; $T_{u,An.}$: analytical ultimate torsional moment.

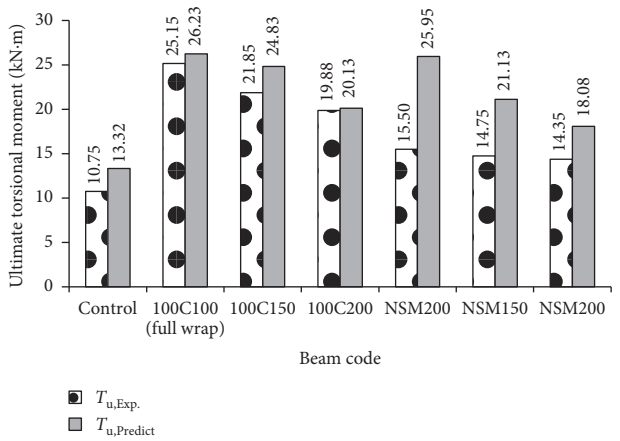

Figure 16: Experimental versus analytical ultimate torsional moments at each concrete beam.

$$T_{u,RC} = T_T + T_L, \tag{10}$$

$$T_T = \frac{2(0.85) \cdot A_o \cdot A_t \cdot f_{yv}}{S}, \tag{10a}$$

$$T_L = \frac{2A_o \cdot A_{sl} \cdot f_{sl}}{P_o} \tan\theta, \tag{10b}$$

$$\tan\theta = \sqrt{\frac{A_t \cdot f_{st} \cdot P_o}{A_{sl} \cdot f_{sl} \cdot S}}. \tag{10c}$$

Equation (10) can also be used to calculate $T_{u,NSM}$ as follows:

$$T_{u,NSM} = \frac{2(0.85) \cdot A_{o,NSM} \cdot A_{t,NSM} \cdot f_{yv,NSM}}{S_{NSM}}. \tag{11}$$

Table 7 and Figure 16 present the comparison of the experimental and the predicted analytical results of the total torsional capacity using ACI 318-14M [67] and FIB Bulletin-14, 2001 [69] design model equations. It was observed that the total torsional capacity was over-estimated by 19% for the control beam. This was due to taking into consideration the effect of longitudinal steel reinforcement (dowel action) contribution to the ultimate torsional moment of reinforced concrete beams.

For strengthened RC beams 100C100, 100C150, and 100C200, the predicted values are in good agreement with the experimental one. However, for the strengthened beam NSM100, NSM150, and NSM200 the predicted values are obviously higher than the experimental values.

5. Conclusions

Apart from the shear and flexural strengths of RC beams, this study also focused on the torsional behaviour of RC beams strengthened with various CFRP wrapping configurations and NSM steel bar under the combined effect of torsion and bending. The following conclusions were obtained from the experimental work:

(i) Despite the CFRP wrapping configurations and NSM steel bar spacing, higher torsional resistance than that of the control beam was observed for all strengthened beams.

(ii) The test beams with CFRP wrapping showed better enhancement in the ultimate torsional moment as opposed to the beams that were strengthened with NSM steel bar. The percentage of enhancement in the ultimate torsional moment (T_u), with respect to control specimen for beams 100C100, 100C150, and 100C200, were 134%, 103%, and 85%, respectively. While this percentage for beams NSM100, NSM150, and NSM200 were 44%, 37%, and 33%, respectively.

(iii) The ductility of all the CFRP-strengthened beams increased; while it decreased for NSM steel bar-strengthened beams. The percentage of enhancement in ultimate twist angle (θ_u), with respect to the control specimen for beams 100C100, 100C150, and 100C200, were 120%, 118%, and 92%, respectively. While the diminution percentage of their ultimate twist angle (θ_u), with respect to the control specimen for beams NSM100, NSM150, and NSM200, were 17%, 24%, and 27%, respectively.

(iv) The enhancement percentage of the ultimate torsional moment (T_u) proportionally increased with increasing of CFRP and NSM steel bar ratio (decreasing the CFRP strip and NSM steel bar spacing).

(v) Cracks in the strengthened beams spread more extensively along their length compared with the singular cracks that formed in the control beam.

(vi) Failure in the concrete beams was delayed when CFRP strip and NSM steel bar were used to strengthen the beams. However, this delay unavoidably occurred in the unwrapped spaces between strips (for CFRP-strengthened beams) and spaces between NSM steel bar grooves (for NSM steel bar-strengthened beams).

(vii) The predicted analytical values for control beam and CFRP-strengthened beams are in good agreement with the experimental one. However, for the NSM steel bar-strengthened beams the predicted values are obviously higher than the experimental one.

Nomenclature

FRP: Fibre-reinforced polymer
CFRP: Carbon fibre-reinforced polymer
GFRP: Glass fibre-reinforced polymer
RC: Reinforced concrete
NSM: Near-surface mounted
A_c: Gross area of the concrete cross section, mm^2
A_{nst}: Area of the NSM steel stirrup reinforcement, mm^2
A_o: Cross-sectional area bounded by the centre line of the shear flow according to ACI 318-14, mm^2
$A_{o,NSM}$: Cross-sectional area bounded by the centre line of the shear flow (NSM-welded steel bar stirrup), mm^2
A_{sl}: Total area of steel longitudinal bars, mm^2
A_t: Area of the transversal steel reinforcement (stirrups), mm^2
$A_{t,NSM}$: Area of the NSM-welded steel reinforcement (stirrups), mm^2
b_f: Width of the CFRP strips, mm
Bxh: Cross section dimensions of beam
E_{fu}: Modulus of elasticity of FRP at ultimate
f'_c: Concrete compressive strength, MPa
f_{st}, f_{sl}: Stresses in the longitudinal and transverse steel reinforcements, MPa
f_{yv}: Yield stress of transversal steel reinforcement, MPa
$f_{yv,NSM}$: Yield stress of the NSM-welded steel reinforcement, MPa
n_f: Number of plies of CFRP sheets
P_f: Perimeter of the strengthened beam cross section using CFRP, mm
P_{nst}: Perimeter of the NSM steel stirrup, mm
P_o: Perimeter of the centerline of the shear flow in space truss analysis, mm
p_t: Perimeter of the steel stirrup, mm
S: Spacing of steel stirrups, mm
S_f: Centre-to-centre spacing of FRP strips, mm
S_n: Centre-to-centre spacing of the NSM steel stirrups, mm
S_{NSM}: Horizontal spacing of the NSM-welded stirrups, mm
T_{cr}: Cracking torque, kN·m
T_L: Torsional contribution of longitudinal steel reinforcement, kN·m
T_T: Torsional contribution of transverse steel reinforcement, kN·m
t_f: Thickness of fibre laminate, mm
t_{fd}: Fabric design thickness, mm
T_u: Ultimate torsional capacity of the strengthened beam, kN·m
$T_{u,An}$: Analytical ultimate torsional moment, kN·m
$T_{u,Exp}$: Experimental ultimate torsional moment, kN·m
$T_{u,FRP}$: Ultimate torsional capacity from FRP reinforcement, kN·m
$T_{u,NSM}$: Ultimate torsional capacity from NSM reinforcement, kN·m
$T_{u,RC}$: Ultimate torsional capacity from steel reinforcement, KN·m
ε_{fe}: Effective FRP strain, mm/mm
$\varepsilon_{fk,e}$: Characteristic value of effective FRP strain, mm/mm
ε_{fu}: Ultimate FRP strain, mm/mm
Θ: Angle of diagonal crack with respect to the member axis, deg
θ_u: Ultimate twist angle, deg
ρ: Total steel reinforcement ratio for each of the longitudinal and transverse reinforcement, mm^2/mm^2
ρ_{nst}: Area of the NSM steel stirrup reinforcement ratio, mm^2/mm^2
ρ_{sl}: Ratio of the longitudinal steel bar, mm^2/mm^2
ρ_{st}: Ratio of transverse steel stirrups, mm^2/mm^2.

Data Availability

The data used to support the findings of this study are included within the article.

Disclosure

The sponsors had no role in the design of the study, in the collection, analyses, or interpretation of data, in the writing of the manuscript, and in the decision to publish the results.

Conflicts of Interest

The authors declare no conflicts of interest.

Authors' Contributions

Both authors conceived and designed the experiments. Nasih Askandar analysed the data and wrote the paper, and Abdulkareem Mahmood made necessary revisions.

Acknowledgments

The authors acknowledge the support provided by Salahaddin University in Erbil and Sulaimani Polytechnic University in Sulaymaniyah.

References

[1] R. Santhakumar, R. Dhanaraj, and E. Chandrasekaran, "Behaviour of retrofitted reinforced concrete beams under combined bending and torsion: a numerical study," *Electronic Journal of Structural Engineering*, vol. 7, pp. 1–7, 2007.

[2] A. Ghobarah, M. N. Ghorbel, and S. E. Chidiac, "Upgrading torsional resistance of reinforced concrete beams using fiber-reinforced polymer," *Journal of Composites for Construction*, vol. 6, no. 4, pp. 257–263, 2002.

[3] American Concrete Institute, *ACI 440.2R-08 Guide for the Design and Construction of Externally Bonded FRP Systems for Strengthening Concrete Structures*, American Concrete Institute, Farmington Hills, MI, USA, 2008.

[4] Ön Anil, "Improving shear capacity of RC T-beams using CFRP composites subjected to cyclic load," *Cement and Concrete Composites*, vol. 28, no. 7, pp. 638–649, 2006.

[5] A. Bousselham and O. Chaallal, "Mechanisms of shear resistance of concrete beams strengthened in shear with externally bonded FRP," *Journal of Composites for Construction*, vol. 12, no. 5, pp. 499–512, 2008.

[6] A. Belarbi, S.-W. Bae, and A. Brancaccio, "Behavior of full-scale RC T-beams strengthened in shear with externally bonded FRP sheets," *Construction and Building Materials*, vol. 32, pp. 27–40, 2012.

[7] N. F. Grace, "Strengthening of negative moment region of reinforced concrete beams using carbon fiber-reinforced polymer strips," *ACI Structural Journal*, vol. 98, no. 3, pp. 347–358, 2001.

[8] A. A. El-Ghandour, "Experimental and analytical investigation of CFRP flexural and shear strengthening efficiencies of RC beams," *Construction and Building Materials*, vol. 25, no. 3, pp. 1419–1429, 2011.

[9] J. F. Bonacci and M. Maalej, "Behavioral trends of RC beams strengthened with externally bonded FRP," *Journal of Composites for Construction*, vol. 5, no. 2, pp. 102–113, 2001.

[10] C. A. Issa and A. AbouJouadeh, "Carbon fiber reinforced polymer strengthening of reinforced concrete beams: experimental study," *Journal of Architectural Engineering*, vol. 10, no. 4, pp. 121–125, 2004.

[11] N. Eshwar, T. James Ibell, and A. Nanni, "Effectiveness of CFRP strengthening on curved soffit RC beams," *Advances in Structural Engineering*, vol. 8, no. 1, pp. 55–68, 205.

[12] K. Soudki, E. El-Salakawy, and B. Craig, "Behavior of CFRP strengthened reinforced concrete beams in corrosive environment," *Journal of Composites for Construction*, vol. 11, no. 3, pp. 291–298, 2007.

[13] M. A. Alam and M. Z. Jumaat, "Eliminating premature end peeling of flexurally strengthened reinforced concrete beams," *Journal of Applied Sciences*, vol. 9, no. 6, pp. 1106–1113, 2009.

[14] H. R. Sobuz and E. Ahmed, "Flexural performance of RC beams strengthened with different reinforcement ratios of CFRP laminates," *Key Engineering Materials*, vol. 471-472, pp. 79–84, 2011.

[15] J. Dong, Q. Wang, and Z. Guan, "Structural behaviour of RC beams with external flexural and flexural-shear strengthening by FRP sheets," *Composites Part B: Engineering*, vol. 44, no. 1, pp. 604–612, 2013.

[16] A. Monier, X. Zhe, H. Huang, and W. Zhishen, "External flexural strengthening of RC beams using BFRP grid and PCM," *Journal of Japan Society of Civil Engineers, Ser. A2 (Applied Mechanics (AM))*, vol. 73, no. 2, pp. I_417–I_427, 2017.

[17] D. Paul and A. Kumar Datta, "A Study on flexural strengthening of RC beam using FRP," in *Proceedings of the International Conference on Advances in Construction Materials and Structures*, pp. 1–9, IIT Roorkee, Uttarakhand, India, 2018.

[18] Y. Murad, "An experimental study on flexural strengthening of RC beams using CFRP sheets," *International Journal of Engineering & Technology*, vol. 7, no. 4, pp. 2075–2080, 2018.

[19] J. Jayaprakash, A. A. Abdul Samad, and A. Anvar Abbasvoch, "Experimental investigation on shear capacity of reinforced concrete precracked push-off specimens with externally bonded bi-directional carbon fibre reinforced polymer fabrics," *Modern Applied Science*, vol. 3, no. 7, pp. 86–98, 2009.

[20] M. B. S. Alferjani, A. A. B. A. Samad, B. S. Elrawaff, N. B. Mohamad, and M. H. B. Ahmad, "Shear strengthening of reinforced concrete beams using carbon fiber reinforced polymer laminate: a review," *American Journal of Civil Engineering*, vol. 2, no. 1, pp. 1–7, 2014.

[21] H. Shariatmadar, M. Khatamirad, and E. Zamani, "Precracked concrete shear strengthened with external CFRP strips," *Civil Engineering*, vol. 1, no. 1, pp. 29–38, 2013.

[22] M. B. S. Alferjani, A. A. A. Samad, B. S. Elrawaff, and N. Mohamad, "Behavior on shear strengthening of precraced/repair RC continuous beams using CFRP strips," *International Journal of Engineering and Science*, vol. 4, no. 5, pp. 32–44, 2014.

[23] N. Ali, A. A. A. Samad, N. Mohamad, and J. Jayaprakash, "Shear behaviour of pre-cracked continuous beam repaired using externally bonded CFRP strips," *Procedia Engineering*, vol. 53, pp. 129–144, 2013.

[24] D. Lavorato, C. Nuti, and S. Silvia, "Experimental investigation of the shear strength of RC beams extracted from an old structure and strengthened by carbon FRP U-strips," *Applied Sciences*, vol. 8, no. 7, Article ID 1182, 2018.

[25] Y. Zhou, M. Guo, L. Sui et al., "Shear strength components of adjustable hybrid bonded CFRP shear-strengthened RC beams," *Composites Part B: Engineering*, vol. 163, pp. 36–51, 2019.

[26] J. A. O. Barros, I. G. Costa, and A. Ventura-Gouveia, "CFRP flexural and shear strengthening technique for RC beams: experimental and numerical research," *Advances in Structural Engineering*, vol. 14, no. 3, pp. 551–571, 2011.

[27] K. Chansawat, T. Potisuk, T. H. Miller, S. C. Yim, and D. I. Kachlakev, "FE models of GFRP and CFRP strengthening of reinforced concrete beams," *Advances in Civil Engineering*, vol. 2009, Article ID 152196, 13 pages, 2009.

[28] W.-T. Jung, J.-S. Park, J.-Y. Kang, and M.-S. Keum, "Flexural behavior of concrete beam strengthened by near-surface mounted CFRP reinforcement using Equivalent section model," *Advances in Materials Science and Engineering*, vol. 2017, Article ID 9180624, 16 pages, 2017.

[29] M. M. Önal, "Strengthening reinforced concrete beams with CFRP and GFRP," *Advances in Materials Science and Engineering*, vol. 2014, Article ID 967964, 8 pages, 2014.

[30] N. Zhuang, H. Dong, D. Chen, and Y. Ma, "Experimental study of aged and Seriously damaged RC beams strengthened using CFRP composites," *Advances in Materials Science and Engineering*, vol. 2018, Article ID 6260724, 9 pages, 2018.

[31] A. M. H. Kadhim, H. A. Numan, and M. Özakça, "Flexural strengthening and rehabilitation of Reinforced concrete beam using BFRP composites: finite element approach," *Advances in Civil Engineering*, vol. 2019, Article ID 4981750, 17 pages, 2019.

[32] V. H. Jariwala, P. V. Patel, and S. P. Purohit, "Strengthening of RC beams subjected to combined torsion and bending with GFRP composites," *Procedia Engineering*, vol. 51, pp. 282–289, 2013.

[33] M. Ameli, H. R. Ronagh, and P. F. Dux, "Behavior of FRP strengthened reinforced concrete beams under torsion," *Journal of Composites for Construction*, vol. 11, no. 2, pp. 192–200, 2007.

[34] C. E. Chalioris, "Torsional strengthening of rectangular and flanged beams using carbon fibre-reinforced-polymer-s—experimental study," *Construction and Building Materials*, vol. 22, no. 1, pp. 21–29, 2008.

[35] M. R. Mohammadizadeh, M. J. Fadaee, and H. R. Ronagh, "Improving torsional behaviour of reinforced concrete beams strengthened with carbon fibre reinforced polymer composite," *Iranian Polymer Journal*, vol. 18, no. 4, pp. 315–327, 2009.

[36] A. Deifalla and A. Ghobarah, "Strengthening RC T-beams subjected to combined torsion and shear using FRP fabrics: experimental study," *Journal of Composites for Construction*, vol. 14, no. 3, pp. 301–311, 2010.

[37] D. Mostofinejad and S. Talaeitaba, "Strengthening and rehabilitation of RC beams with frp overlays under combined shear and torsion," *Electronic Journal of Structural Engineering*, vol. 14, pp. 84–92, 2014.

[38] U. A. Kumar, V. Bhargavi, and E. V. R. Rao, "Study of torsional behaviour of rectangular reinforced concrete beams wrapped with GFRP," *International Journal of Research Publications in Engineering and Technology [IJRPET]*, vol. 2, no. 1, pp. 1–6, 2015.

[39] P. V. Patel, V. H. Jariwala, and S. P. Purohit, "Torsional strengthening of RC beams using GFRP composites," *Journal of The Institution of Engineers (India): Series A*, vol. 97, no. 3, pp. 313–322, 2016.

[40] A. K. S. Soluit, "Torsional behavior of RC beams strengthened with fiber reinforced polymer sheets," *Engineering Research Journal*, vol. 114, pp. 102–119, 2007.

[41] L. De Lorenzis and J. G. Teng, "Near-surface mounted FRP reinforcement: an emerging technique for strengthening structures," *Composites Part B: Engineering*, vol. 38, no. 2, pp. 119–143, 2007.

[42] A. Mofidi, O. Chaallal, L. Cheng, and Y. Shao, "Investigation of near surface–mounted method for shear rehabilitation of reinforced concrete beams using fiber reinforced–polymer composites," *Journal of Composites for Construction*, vol. 20, no. 2, Article ID 04015048, 2015.

[43] M. Ramezanpour, R. Morshed, and A. Eslami, "Experimental investigation on optimal shear strengthening of RC beams using NSM GFRP bars," *Structural Engineering Mechanics*, vol. 67, no. 1, pp. 45–52, 2018.

[44] B. Almassri, "Strengthening of corroded reinforced concrete (RC) beams with near surface mounted (NSM) technique using carbon fiber polymer (CFRP) rods; an experimental and finite element (FE) modelling study," INSA Toulouse, Toulouse, France, Theses, 2015.

[45] G. Wu, Z.-Q. Dong, Z.-S. Wu, and L.-W. Zhang, "Performance and parametric analysis of flexural strengthening for RC beams with NSM-CFRP bars," *Journal of Composites for Construction*, vol. 18, no. 4, Article ID 04013051, 2013.

[46] I. A. Sharaky, L. Torres, J. Comas, and C. Barris, "Flexural response of reinforced concrete (RC) beams strengthened with near surface mounted (NSM) fibre reinforced polymer (FRP) bars," *Composite Structures*, vol. 109, pp. 8–22, 2014.

[47] N. Kishi, H. Mikami, Y. Kurihashi, and S. Sawada, "Flexural behaviour of RC beams reinforced with NSM AFRP rods," in *Proceedings of the International Symposium on Bond Behaviour of FRP in Structures (BBFS 2005)*, Hong Kong, China, December 2005.

[48] S. Gopinath, A. R. Murthy, and H. Patrawala, "Near surface mounted strengthening of RC beams using basalt fiber reinforced polymer bars," *Construction and Building Materials*, vol. 111, pp. 1–8, 2016.

[49] F. Al-Mahmoud, A. Castel, R. François, and C. Tourneur, "RC beams strengthened with NSM CFRP rods and modeling of peeling-off failure," *Composite Structures*, vol. 92, no. 8, pp. 1920–1930, 2010.

[50] I. A. Sharaky, R. M. Reda, M. Ghanem, M. H. Seleem, and H. E. M. Sallam, "Experimental and numerical study of RC beams strengthened with bottom and side NSM GFRP bars having different end conditions," *Construction and Building Materials*, vol. 149, pp. 882–903, 2017.

[51] J. Barros, S. Dias, and A. Fortes, "Near surface mounted technique for the flexural and shear strengthening of concrete beams," in *Proccedings of the International Conference on Concrete for Structures*, pp. 229–236, University of Coimbra, Scotland, UK, 2005.

[52] R. El-Hacha and M. Gaafar, "Flexural strengthening of reinforced concrete beams using prestressed, near-surface-mounted CFRP bars," *PCI Journal*, vol. 56, no. 4, pp. 134–151, 2011.

[53] M. A. Hosen, U. J. Alengaram, M. Z. Jumaat, and N. H. R. Sulong, "Glass Fiber Reinforced Polymer (GFRP) bars for enhancing the flexural performance of RC beams using side-NSM technique," *Polymers*, vol. 9, no. 12, p. 180, 2017.

[54] S. S. Zhang, T. Yu, and G. M. Chen, "Reinforced concrete beams strengthened in flexure with near-surface mounted (NSM) CFRP strips: current status and research needs," *Composites Part B: Engineering*, vol. 131, pp. 30–42, 2017.

[55] A. A. Shukri, M. A. Hosen, R. Muhamad, and M. Z. Jumaat, "Behaviour of precracked RC beams strengthened using the side-NSM technique," *Construction and Building Materials*, vol. 123, pp. 617–626, 2016.

[56] A. Ghanim and B. Al-Abbas, "Experimental study on the flexural strengthening of reinforced concrete beams using NSM CFRP bars," in *Proceedings of the 5th National and 1st International Conference on Modern Materials and Structures in Civil Engineering*, At Amirkabir University of Technology, Tehran-Iran, 2018.

[57] K. Heiza, N. N. Meleka, and N. Y. Elwkad, "Behavior and analysis of Self-Consolidated reinforced concrete deep beams strengthened in shear," *ISRN Civil Engineering*, vol. 2012, Article ID 202171, 14 pages, 2012.

[58] W.-T. Jung, J.-S. Park, J.-Y. Kang, and H. B. Park, "Strengthening effect of prestressed near-surface-mounted CFRP Tendon on reinforced concrete beam," *Advances in Materials Science and Engineering*, vol. 2018, Article ID 9210827, 18 pages, 2018.

[59] H. H. Kammona and A. S. H. Al-Issawi, "Estimation of maximum shear capacity of RC deep beams strengthened by NSM steel bars," *Journal of University of Babylon*, vol. 26, no. 3, pp. 13–22, 2018.

[60] N. Franco, H. Biscaia, and C. Chastre, "Experimental and numerical analyses of flexurally-strengthened concrete T-beams with stainless steel," *Engineering Structures*, vol. 172, pp. 981–996, 2018.

[61] M. A. Hosen, M. Z. Jumaat, K. M. U. Darain, M. Obaydullah, and A. B. M. Saiful Islam, "Flexural strengthening of RC beams with NSM steel bars," in *Proceedings of the International Conference on Food, Agriculture and Biology*, Kuala Lumpur, Malaysia, June 2014.

[62] M. Breveglieri, A. Aprile, and J. A. O. Barros, "Shear strengthening of reinforced concrete beams strengthened using embedded through section steel bars," *Engineering Structures*, vol. 81, pp. 76–87, 2014.

[63] K. N. Rahal and H. A. Rumaih, "Tests on reinforced concrete beams strengthened in shear using near surface mounted CFRP and steel bars," *Engineering Structures*, vol. 33, no. 1, pp. 53–62, 2011.

[64] M. Hosen, M. Jumaat, U. Alengaram, A. Islam, and H. Bin Hashim, "Near surface mounted composites for flexural strengthening of reinforced concrete beams," *Polymers*, vol. 8, no. 3, p. 67, 2016.

[65] G. Al-Bayati, R. Al-Mahaidi, and R. Kalfat, "Experimental investigation into the use of NSM FRP to increase the

torsional resistance of RC beams using epoxy resins and cement-based adhesives," *Construction and Building Materials*, vol. 124, pp. 1153–1164, 2016.

[66] G. Al-Bayati, R. Al-Mahaidi, M. J. Hashemi, and R. Kalfat, "Torsional strengthening of RC beams using NSM CFRP rope and innovative adhesives," *Composite Structures*, vol. 187, pp. 190–202, 2018.

[67] American Concrete Institute, *ACI.318M-14 Building Code Requirements for Structural Concrete*, American Concrete Institute, Farmington Hills, MI, USA, 2014.

[68] C. E. Chalioris and C. G. Karayannis, "Experimental investigation of RC beams with rectangular spiral reinforcement in torsion," *Engineering Structures*, vol. 56, pp. 286–297, 2013.

[69] Fédération Internationale Du béton, *Externally Bonded FRP Reinforcement for RC Structures*, Fédération Internationale Du béton, Lausanne, Switzerland, 2001.